

In Situ Formation of Thermosensitive PNIPAAm-Based Hydrogels by Michael-Type Addition Reaction

Zong-Chun Wang,^{†,‡} Xiao-Ding Xu,[†] Chang-Sheng Chen,[†] Liu Yun,[†] Jin-Chun Song,[‡] Xian-Zheng Zhang,^{*,†} and Ren-Xi Zhuo[†]

Key Laboratory of Biomedical Polymers of Ministry of Education & Department of Chemistry, Wuhan University, Wuhan 430072, P. R. China, and Department of Pharmacy, Renmin Hospital of Wuhan University, Wuhan 430060, P. R. China

ABSTRACT To investigate the possibility of in situ thermosensitive hydrogel formation via Michael-type addition reaction, we designed and prepared thiol- and vinyl-modified poly(*N*-isopropylacrylamide) (PNIPAAm)-based copolymers. When the solutions of these two kinds of PNIPAAm-based copolymers were mixed at physiological temperature (37 °C), a physical gelation resulting from the hydrophobic aggregation of PNIPAAm based copolymers and chemical cross-linking between thiol and vinyl functional groups or so-called chemical gelation occurred, resulting in the formation of a three-dimensional hydrogel. Because all the gelations were performed at a high temperature (above LCSTs of the PNIPAAm based copolymers), these in situ formed hydrogels presented heterogeneous network structures, resulting in an improved thermosensitivity in comparison with the conventional one.

KEYWORDS: Michael addition • in situ • hydrogel • thermosensitivity

INTRODUCTION

Because of the enormous potential in various applications in the biochemical and biomedical fields, hydrogels that can swell in water and hold a large amount of water while maintaining their chemical structures have been widely explored (1–4). The most common synthesis of cross-linked hydrogels involves the polymerization of water-soluble vinyl monomers in the presence of cross-linkers and initiators (5–7). In recent years, hydrogels that can be formed in situ under physiological conditions have drawn much attention because of their favorable characteristics. Therapeutic drugs or cells or both can be mixed with the polymer solution prior to gelation, and the in situ gelation allows the formation of complicated shapes and could be administrated through minimally invasive surgery (8–10).

Generally, the in situ formed hydrogels can be divided into two types: physical and chemical patterns. In the past few decades, the physically cross-linked hydrogels have been well-studied based on the stimuli-responsive block copolymers such as poly(ethylene oxide)-poly(propylene oxide)-poly(ethylene oxide) (PEO-PPO-PEO) triblock copolymer (11, 12). Recently, inclusion complexation (13), β -sheet or coiled-coil formation of peptides (14) and stereocomplexation between poly(L-lactide) and poly(D-lactide) (15) have been also developed for the in situ formation of physically cross-linked hydrogels. A major drawback of physically

cross-linked hydrogels is the weak mechanical strength (16). Being different from the physically cross-linked hydrogels, the mechanical strength of chemical cross-linked hydrogels is improved dramatically because of the presence of chemical cross-linking joints. The most common chemically cross-linked hydrogels are prepared via UV irradiation of (meth)acrylate functionalized polymers (17–19). However, in vivo applications of these in situ formed hydrogels are limited because of the low penetration depth of UV light (16). Actually, besides UV irradiation, some other chemoselective cross-linking reactions initiated by simply mixing the polymer solutions have been established for the hydrogels of in situ formations. For example, coupling reaction between an aldehyde and a hydrazide group (20, 21) or a cysteine 1,2-aminothiol group (22) and nucleophilic substitution reaction between epoxy and amine groups (23). Besides, “click” chemistry, a type of Huisgen’s 1,3-dipolar azide–alkyne cycloaddition with the unique properties including high specificity, quantitative yield, and near-perfect fidelity was also developed for in situ formation of hydrogels (24–26).

In recent years, as a popular strategy, Michael addition chemistry between thiols and either acrylates or vinyl sulfones has been employed for in situ formation of hydrogels (16, 27–30). This reaction is highly selective and can be carried out under physiological conditions, providing a promise to prepare biomimetic scaffolds via the incorporation of thiol-bearing biomolecules. Hubbell et al. reported several in situ formed hydrogels by Michael addition chemistry between multifunctional poly(ethylene glycol) (PEG) vinyl sulfones or acrylates and multifunctional thiol compounds (27–30). It was found that the release of bovine serum albumin (BSA) from these hydrogels presented zero-

* Corresponding author. Tel./fax: +86-27-68754509. E-mail: xz-zhang@whu.edu.cn.

Received for review October 19, 2009 and accepted March 3, 2010

[†] Wuhan University.

[‡] Renmin Hospital of Wuhan University.

DOI: 10.1021/am900712e

2010 American Chemical Society

order kinetics (27). To date, numerous *in situ* formed hydrogels including cell-responsive PEG-based hydrogels (29) and biodegradable dextran-based hydrogels (16, 30) have been prepared by Michael addition chemistry and applied for drug delivery and tissue scaffolds (31). However, environmental sensitive hydrogels formed via Michael addition chemistry are seldom reported (32–34). It is known that environmental sensitive hydrogels can respond and change their shapes and volumes upon external stimuli including pH (35), temperature (36), and photo field (37). Especially for the thermosensitive ones, because the network structures can be easily adjusted via altering the external temperature, these hydrogels present potential advantages in many fields, such as protein–ligand recognition (38), on–off switches for modulated drug delivery (39), and immobilization of enzyme (40). Hoffman et al. (41) and Kim et al. (42) indicated that the thermosensitive hydrogels can be used as on–off drug release patterns in response to a stepwise temperature change. This subject has been also reviewed in some recent reviews (1, 43). In this study, the most popular thermosensitive poly(*N*-isopropylacrylamide) (PNIPAAm) was selected for the purpose of *in situ* hydrogel formation via Michael-type addition reaction. On the basis of this point, two types of PNIPAAm-based copolymers, thiol-modified P(NIPAAm-*co*-NAS) and vinyl-modified P(NIPAAm-*co*-HEMA), were designed and prepared. When the solutions of these two types of copolymers were mixed and placed at physiological temperature (37 °C), a temperature triggered physical gelation resulting from the hydrophobic aggregation of PNIPAAm segments in the polymeric chains appeared immediately. Combined with the cross-linking reaction between thiol and vinyl functional groups or so-called Michael-type addition reaction, a physically and chemically cross-linked hydrogel was ultimately formed, which exhibited an improved thermosensitivity in comparison with the conventional one.

MATERIALS AND METHODS

Materials. *N*-Isopropylacrylamide (NIPAAm) and 2-amino ethanethiol hydrochloride (AET.HCl) were purchased from ACROS and used as received. Fish DNA (M_w = 20 000, total impurities \leq 1% protein, loss \leq 8% loss on drying) was provided by GIBCO Invitrogen Co. and used directly. *N*-Hydroxysuccinimide (NHS), acryloyl chloride, dithiothreitol (DTT) and dimethylformamide (DMF) were obtained from Shanghai Reagent Chemical Co. (China) and used without further purification. *N,N*'-Azobisisobutyronitrile (AIBN) was purchased from Shanghai Reagent Chemical Co. (China) and recrystallized from ethanol. Hydroxylethyl methacrylate (HEMA), chloroform, tetrahydrofuran (THF) and triethylamine (TEA) were provided by Shanghai Chemical Reagent Co. (China) and distilled before use. All other reagents were of analytical grade and used without further purification.

Synthesis of *N*-Acryloxy succinimide (NAS). *N*-Acryloxy succinimide (NAS) was synthesized via a substitution reaction between *N*-hydroxysuccinimide (NHS) and acryloyl chloride in the presence of triethylamine. Briefly, 50 mL of anhydrous chloroform, NHS (4.25 g, 36.9 mmol), and triethylamine (6.5 mL, 41.9 mmol) were added to a flask cooled in an ice-salt bath. Acryloyl chloride (3.5 mL, 38.7 mmol) which was diluted in 15 mL of chloroform was added dropwise to the flask. After the addition, the flask was sealed and the mixture was allowed to stir for another 3 h in the ice-salt bath. Thereafter, the solution

Table 1. Feed Compositions of PNIPAAm-Based Copolymers

	monomers (mmol)	yield				M_n^a	PDI	MR ^b
		no.	NIPAAm	NAS	HEMA	(%)		
P(NIPAAm- <i>co</i> -NAS)	1	40	4.44			80.3	25 000	1.70
	2	40	3.33			83.7	25 600	1.57
P(NIPAAm- <i>co</i> -HEMA)	3	40		4.44		75.3	32 100	1.87
	4	40		3.33	79.1	26 300	1.91	12.2:1

^a Determined by GPC measurement. ^b Molar ratio of NIPAAm units to NAS units in P(NIPAAm-*co*-NAS) or NIPAAm units to HEMA units in P(NIPAAm-*co*-HEMA) calculated from the ¹H NMR spectra.

was washed twice with 30 mL of saturated brine, dried with MgSO₄, and filtered. The filtration was subsequently concentrated to obtain a crude product. The purified NAS was collected via recrystallization in a mixture of *n*-hexane (30 mL) and ethyl acetate (10 mL). ¹H NMR (300 MHz, CDCl₃, δ ppm): 6.66–6.74 (CH₂=CHC=O, 1H, trans), 6.26–6.38 (CH₂=CHC=O, 1H, cis), 6.14–6.18 (CH₂=CHC=O, 1H), 2.86 (O=CCH₂CH₂C=O, 4H).

Preparation of P(NIPAAm-*co*-NAS). NIPAAm and NAS with different molar ratios (9:1 and 12:1) and a particular amount of AIBN as initiator (1 mol % based on the total monomers) were dissolved in anhydrous DMF. The solution was degassed by bubbling with nitrogen for 30 min. The mixture was reacted at 70 °C for 24 h under nitrogen. The product was then precipitated in cold diethyl ether thrice. After the precipitation and drying in a vacuum for 24 h, a colorless product was collected. The detailed feed compositions are summarized in Table 1.

Preparation of P(NIPAAm-*co*-HEMA). NIPAAm and HEMA with different molar ratios (9:1 and 12:1) and a particular amount of AIBN as initiator (1 mol % based on the total monomers) were dissolved in anhydrous DMF. The solution was degassed by bubbling with nitrogen for 30 min and then reacted at 70 °C for 24 h under nitrogen. The product was collected after the precipitation in cold diethyl ether thrice and drying in vacuum. The detailed feed compositions can be found in Table 1.

Preparation of Thiol-Modified P(NIPAAm-*co*-NAS). Three grams of P(NIPAAm-*co*-NAS) and particular amount of AET.HCl (10-fold molar excess compared to the amount of NAS moieties of P(NIPAAm-*co*-NAS)) were dissolved in 20 mL of anhydrous THF. The solution was degassed by bubbling with nitrogen for 30 min. Thereafter, 1.5 mL triethylamine (TEA) was added to deprotect hydrochloride and the reaction was performed at room temperature for 24 h under a nitrogen atmosphere. Subsequently, DTT (equal amount to AET.HCl used) was added to disrupt disulfide bonds. The product was collected after the precipitation in cold diethyl ether thrice and drying in a vacuum.

Preparation of Vinyl-Modified P(NIPAAm-*co*-HEMA). Three grams of P(NIPAAm-*co*-HEMA) and 1.5 mL of triethylamine were dissolved in 20 mL of anhydrous THF. Under an ice-salt bath, acryloyl chloride (10-fold molar excess compared to the amount of HEMA moieties of P(NIPAAm-*co*-HEMA)) diluted in 5 mL of THF was added dropwise to the solution in dark. Thereafter, the mixture was allowed to stir at room temperature in dark for another 12 h. After triethylammonium chloride salt was removed via filtration, the product was obtained via the precipitation in cold diethyl ether thrice and drying in vacuum.

Gel Permeation Chromatography (GPC). Number- and weight-average molecular weights (M_n and M_w , respectively) of the PNIPAAm-based copolymers (dissolving in THF at a concentration of 5 mg/mL) were determined by a gel permeation chromatographic system equipped with Waters 2690D separations module, Waters 2410 refractive index detector. THF was used as the mobile phase at a flow rate of 0.3 mL/min. Waters millennium module software was used to calculate molecular

Table 2. Feed Compositions, Gelation Time, Gelation Temperature and Maximum Storage of the In situ Formed PNIPAAm-Based Hydrogels

	Sample ID			
	Gel13	Gel14	Gel23	Gel24
thiol-modified P(NIPAAm- <i>co</i> -NAS) ^a	1'	1'	2'	2'
vinyl-modified P(NIPAAm- <i>co</i> -HEMA) ^b	3'	4'	3'	4'
gelation time (s) ^c	25	38	34	37
G' (Pa) ^d	1506.9	1107.3	1127.4	840.1

^a 1' and 2' are thiol-modified P(NIPAAm-*co*-NAS) prepared from 1 and 2 in Table 1. ^b 3' and 4' are vinyl-modified P(NIPAAm-*co*-HEMA) prepared from 3 and 4 in Table 1. ^c Determined by time sweeps. ^d The maximum value of the storage modulus determined by frequency sweeps.

weight on the basis of a universal calibration curve generated by polystyrene standard of narrow molecular weight distribution. Before the GPC measurements, the copolymers were dialyzed in water for 1 week by using dialysis membrane with a molecular weight cutoff 8000–12000. During this period, water was refreshed every day and the purified copolymers were harvested via freeze-drying in a Freeze Drier (Labconco, CA).

¹H NMR. The ¹H NMR spectra of the PNIPAAm based copolymers were recorded on a Mercury VX-300 spectrometer at 300 MHz (Varian) by using CDCl₃ as a solvent and TMS as an internal standard.

LCST Determination. The optical absorbances of the aqueous solutions of thiol-modified P(NIPAAm-*co*-NAS) (0.5 mg/mL) and vinyl-modified P(NIPAAm-*co*-HEMA) (0.5 mg/mL) at various temperatures were measured at 542 nm using a Lambda Bio40 UV-vis spectrometer (Perkin-Elmer). Sample cells were thermostatted in a refrigerated circulator bath at different temperatures from 8 to 48 °C prior to measurements. The heating rate was set at 0.1 °C/min. The LCSTs of the PNIPAAm copolymers were defined as the temperature showing a 50% change in the total optical absorbance.

In situ Hydrogel Formation via Michael-Type Addition Reaction. 50 mg Thiol-modified P(NIPAAm-*co*-NAS) was dissolved in 1 mL PBS to form a 5-wt % homogeneous solution. And another 5 wt % vinyl-modified P(NIPAAm-*co*-HEMA) aqueous solution was also prepared by dissolving 50 mg the copolymer in 1 mL PBS. Then, these two solutions were quickly mixed (within 5 s). After the vortexing at room temperature for 2 min, the mixed solution was placed in an oil bath at 37 °C for 24 h to carry out the gelation. The resulting hydrogel was taken out and immersed in PBS for 3 days to extract the residue. During this process, PBS was refreshed every 4 h. The hydrogel was then immersed in distilled water for another 3 days. The purified hydrogels were cut into disklike pieces approximately 10 mm in diameter and 6 mm in thickness and swollen in distilled water at room temperature for the following characterizations. The detailed feed compositions are summarized in Table 2.

Oscillatory Rheology. Rheology experiments were performed on ARES-RFS III rheometer (TA Instruments, USA). Prior to performing the rheology measurements, the aqueous solutions of thiol-modified P(NIPAAm-*co*-NAS) (5-wt %) and vinyl-modified P(NIPAAm-*co*-HEMA) (5-wt %) were prepared as described above. To examine the time-dependent gelation behaviors of in situ formed hydrogels via Michael-type addition reaction, equal volumes of the aqueous solutions of thiol-modified P(NIPAAm-*co*-NAS) and vinyl-modified P(NIPAAm-*co*-HEMA) were mixed and vortexed at room temperature for 2 min, and the time sweeps were then carried out at 37 °C for 40 min with a constant shear frequency (1 Hz) and strain (10%) after quickly transferring the mixed solution to the rheometer. To investigate the temperature-dependent gelation behaviors of the in situ formed hydro-

gels, we performed the temperature sweeps from 15 to 50 °C with a heating rate of 0.5 °C/min at a constant shear frequency (1 Hz) and strain (10%). After the gelation in the time sweeps described above, the frequency sweeps at 37 °C were subsequently performed from 0.1 to 100 Hz with a constant strain (10%) to study the mechanical strength of in situ formed hydrogels via Michael-type addition reaction.

Interior Morphology. The swollen hydrogel samples were quickly frozen in liquid nitrogen and then freeze-dried in a freeze drier (Labconco, CA) under a vacuum at -45 °C for 3 days. The freeze-dried samples were then fractured carefully in liquid nitrogen, and the interior morphology of hydrogel samples was examined at room temperature by using a scanning electron microscope (SEM, FEI-QUANTA 200, Holland) with an accelerating voltage of 25 kv, work distance of 25.7 mm, and magnification of 3000 \times . Before SEM observation, the hydrogel specimens were coated with gold for 7 min.

Equilibrium Swelling Ratio at Different Temperature. The temperature dependence of equilibrium swelling ratios of the in situ formed hydrogels was studied gravimetrically over a temperature range from 5 to 60 °C. The swollen hydrogel samples were immersed in the distilled water for 24 h at each predetermined temperature by a thermostatted water bath. The samples were blotted with moistened filter paper to remove the excess water on the hydrogel surfaces and weighed. Thereafter, the samples were equilibrated in distilled water again at another predetermined temperature and then the wet weight was determined as mentioned above. The experiments were performed for three times and the average value of three measurements was taken. The dry weights of samples were obtained after dried in vacuum at 45 °C for 24 h. Equilibrium swelling ratio at each temperature was defined as follows

$$SR_{eq} = (W_w - W_d)/W_d \quad (1)$$

where W_w is the wet weight of the swollen hydrogel sample at each temperature and W_d is the dry weight of the hydrogel sample.

Shrinking Kinetics at 45 °C. The shrinking kinetics of the swollen hydrogel samples was measured gravimetrically in distilled water at 45 °C. At predetermined time intervals, the samples were taken from the hot water and weighed after removing the excess water on the surfaces with wet filter paper. Similarly, each sample was measured three times and the average value of three measurements was recorded. Water retention was defined as follows

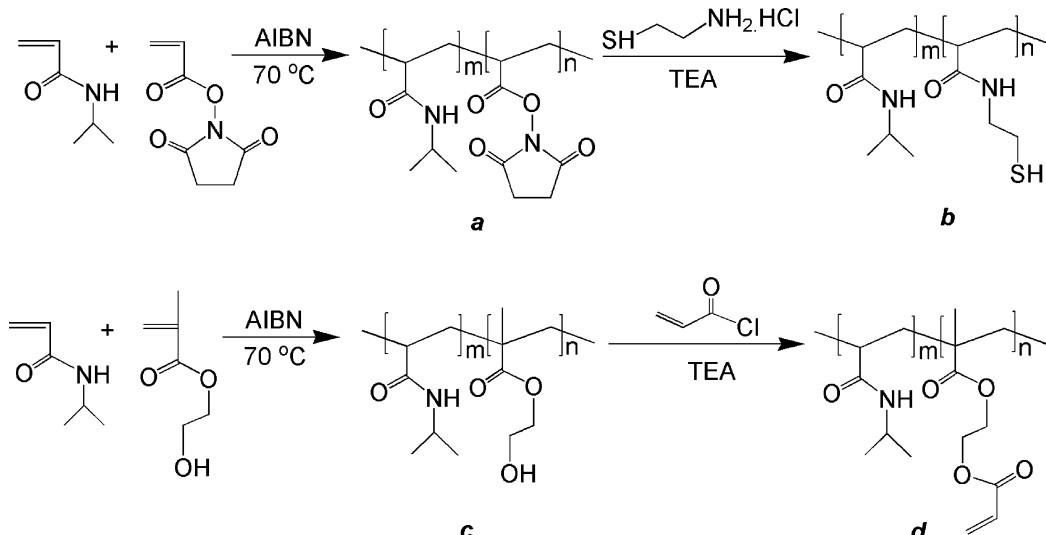
$$[\text{water retention}]_t = [(W_t - W_d)/W_s] \times 100 \quad (2)$$

where W_t is the weight of the wet hydrogel at time t at 45 °C, W_s is the water weight of the swollen hydrogel sample at room temperature, and W_d is the dry weight of the hydrogel sample.

Swelling Kinetics at 22 °C. The swollen hydrogel samples were shrunk in distilled water at 60 °C for 4 h to reach stable state (losing at least 80% water). Then the shrunk samples were immersed in the distilled water at room temperature (22 °C) and removed from water at regular time intervals. After removing the water on the surfaces with wet filter paper, the weight that was the average value of three measurements was recorded. The water uptake at time t was defined as follows

$$[\text{water uptake}]_t = [(W_t - W_d)/W_s] \times 100 \quad (3)$$

where W_t is the weight of the wet hydrogel sample at time t at room temperature, W_s is the water weight of the swollen

Scheme 1. Synthesis Routes of Thiol-Modified P(NIPAAm-*co*-NAS) (b) and Vinyl-Modified P(NIPAAm-*co*-HEMA) (d)

hydrogel sample at room temperature, and W_d is the dry weight of the hydrogel sample.

Drug Loading and In vitro Release. To examine the smart controlled release behaviors of the in situ formed hydrogels, fish DNA was used as a model drug. Fish DNA (30 mg) was thoroughly dissolved in 50 mL of PBS (pH7.4) to form a 0.06-wt % homogeneous solution. Then, 50 mg of thiol-modified P(NIPAAm-*co*-NAS) was dissolved in 1 mL of fish-DNA-loaded PBS to form a 5 wt % homogeneous solution. Another 5 wt % vinyl-modified P(NIPAAm-*co*-HEMA) aqueous solution was also prepared by dissolving 50 mg of the copolymer in 1 mL of fish-DNA-loaded PBS. Then, these two solutions were quickly mixed (within 5 s) in a glass tube. After the vortexing at room temperature for 2 min, the mixed solution was placed in an oil bath at 37 °C for 24 h to carry out the gelation. After the gelation, the hydrogel was taken out from the glass tube for the following drug release study. The fish DNA encapsulation efficiency (EE %) was calculated as

$$\text{EE \%} = M_{\infty}/M_f \times 100 \quad (4)$$

where M_{∞} is the amount of fish DNA loaded in the hydrogel (feed amount of fish DNA-unloaded amount of fish DNA) and M_f is the feed amount of fish DNA.

The in vitro release was carried out at 22 and 37 °C, respectively, to investigate the influence of temperature on fish DNA release. The fish DNA loaded hydrogel sample was immersed in a tube filled with 4 mL of PBS at 22 (below LCST) and 37 °C (above LCST). At a predetermined time interval, the total PBS in the tube was withdrawn and an extra 4 mL of fresh PBS was added after each sampling. The amount of fish DNA released from the hydrogel sample was collected by examining the absorbance of the each withdrawn PBS on a UV spectrophotometer (Perkin-Elmer Lambda Bio 40 UV/vis spectrometer) at 260 nm. The cumulative drug release was calculated as follows

$$\text{cumulative amount released (\%)} = (M_t/M_{\infty}) \times 100 \quad (5)$$

where M_t is the amount of fish DNA released from the hydrogel sample at time t and M_{∞} is the amount of fish DNA loaded in the hydrogel sample.

RESULTS AND DISCUSSION

Synthesis of PNIPAAm-Based Polymers. To investigate the possibility of in situ thermosensitive hydrogel formation via Michael-type addition reaction, thiol and vinyl functional groups were introduced to the structures of PNIPAAm based polymers. As shown in Scheme 1, two precursors, P(NIPAAm-*co*-NAS) (a) and P(NIPAAm-*co*-HEMA) (c), were first synthesized via free radical polymerization. The detailed compositions as well as the molecular weight information are listed in Table 1. To determine the molar ratio of NIPAAm units to NAS or HEMA units in the polymeric chain, we carried out ¹H NMR measurements and the corresponding spectra are exhibited in Figure 1. As for P(NIPAAm-*co*-NAS) (Figure 1A), the chemical shift appearing at $\delta = 4.01$ ppm (signal 6) mainly corresponded to the methylidyne protons adjacent to the amide moieties (CH=NH, 1H) of NIPAAm units. And other signals of NIPAAm units were coincided with our previous studies (5, 25, 26). The chemical shift of methylene protons ($\text{O}=\text{CCH}_2\text{CH}_2\text{C=O}$),

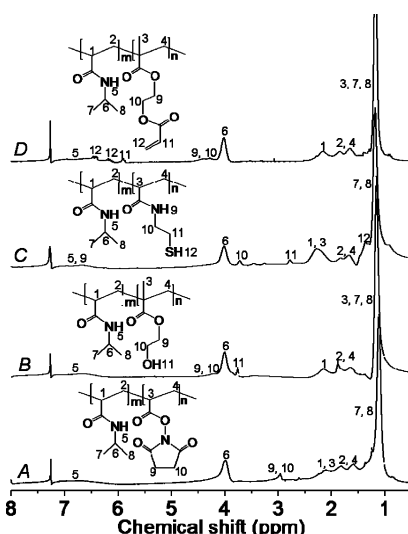


FIGURE 1. ¹H NMR spectra of PNIPAAm based copolymers. (A) P(NIPAAm-*co*-NAS); (B) P(NIPAAm-*co*-HEMA); (C) thiol-modified P(NIPAAm-*co*-NAS); (D) vinyl-modified P(NIPAAm-*co*-HEMA).

4H) of NAS units appeared at 2.97 ppm (signals 9 and 10), which was also accordant with a previous report (34). Here, the molar ratio of NIPAAm units to NAS units in the polymeric chain was calculated from the integration at the chemical shifts 4.01 and 2.97 ppm. In the case of P(NIPAAm-*co*-HEMA) (Figure 1B), the chemical shift of the methylidyne protons adjacent to the amide moieties ($\text{CH}-\text{NH}$, 1H) of NIPAAm units appeared at 3.98 ppm (signal 6). And the chemical shift appearing at 4.23 ppm (signals 9 and 10) mainly corresponded to the methylene protons ($\text{OCH}_2\text{CH}_2\text{O}$, 4H) of HEMA units (25, 26). Similarly as P(NIPAAm-*co*-NAS), the integrations at the chemical shifts 3.98 and 4.23 ppm were selected to calculate the molar ratio of NIPAAm units to HEMA units in the polymeric chain. As exhibited in Table 1, the molar ratio of NIPAAm units to NAS units in P(NIPAAm-*co*-NAS) or NIPAAm units to HEMA units in P(NIPAAm-*co*-HEMA) was almost consistent with their feed compositions.

The substitution reaction was used to synthesize thiol-modified P(NIPAAm-*co*-NAS) (*b*) and vinyl-modified P(NIPAAm-*co*-HEMA) (*d*), respectively. And the corresponding chemical structures were characterized by ^1H NMR to determine the existence of thiol and vinyl functional groups. With respect to the thiol-modified P(NIPAAm-*co*-NAS) (Figure 1C), the typical signals of the methylene protons of cysteamine appeared at 3.68 ppm ($\text{O}=\text{CNHCH}_2\text{CH}_2\text{SH}$, 2H, signal 10) and 2.73 ($\text{O}=\text{CNHCH}_2\text{CH}_2\text{SH}$, 2H, signal 11). Moreover, there were no the chemical signals of NAS units in the spectrum of thiol-modified P(NIPAAm-*co*-NAS), suggesting almost complete conversion of NAS units after the substitution reaction. As for the vinyl-modified P(NIPAAm-*co*-HEMA) (Figure 1D), the chemical shifts appearing at 6.42 ppm ($\text{CH}_2=\text{CHC=O}$, 1H, trans, signal 12), 6.15 ppm ($\text{CH}_2=\text{CHC=O}$, 1H, cis, signal 12), and 5.91 ppm ($\text{CH}_2=\text{CHC=O}$, 1H, signal 11) indicated the existence of vinyl functional groups in the polymeric chain, providing the chance to carry out Michael addition chemistry with thiol-modified P(NIPAAm-*co*-NAS).

LCST Behaviors. It is known that PNIPAAm is a kind of thermosensitive polymer presenting a lower critical solution temperature (LCST) of ~ 32 $^{\circ}\text{C}$ in aqueous solution (44–46). At a temperature below LCST, PNIPAAm can dissolve in aqueous solution. But it undergoes an abrupt phase transition above the LCST, which is associated with precipitation of the polymer. This phase transition of PNIPAAm in aqueous solution is attributed to a change in the hydrophilic/hydrophobic equilibrium of the polymer with respect to the hydrogen bonding interactions between the polymeric chain and water molecules (44, 45). If hydrophilic or hydrophobic moiety was incorporated into PNIPAAm polymeric chain, the resulted polymer will be more hydrophilic or hydrophobic and thus, the corresponding LCST will shift to a higher or lower value. In this study, in order to examine the LSCT behaviors of the thiol-modified P(NIPAAm-*co*-NAS) and vinyl-modified P(NIPAAm-*co*-HEMA), the optical absorbances of the aqueous solutions of the copolymers were examined and exhibited Figure 2. It was found that all the solutions of the copolymers had an abrupt change of

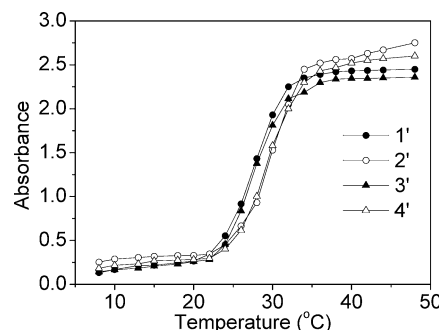
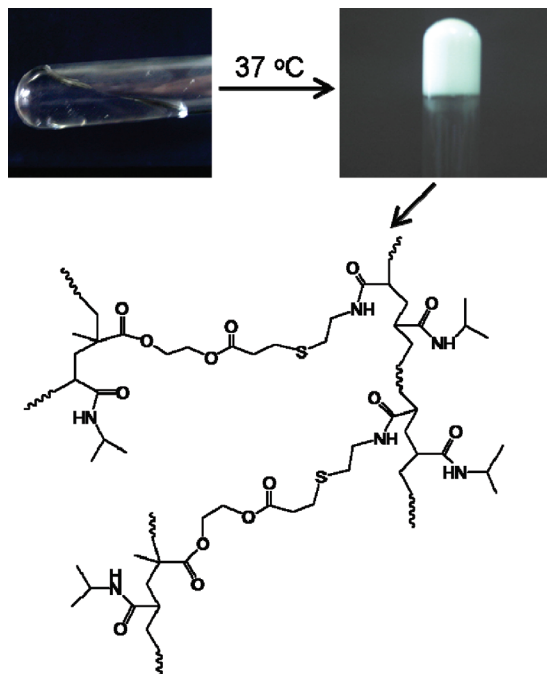


FIGURE 2. LCSTs of the thiol-modified P(NIPAAm-*co*-NAS) (1' and 2') and vinyl-modified P(NIPAAm-*co*-HEMA) (3' and 4').

optical absorbance in the temperature range from 20 to 35 $^{\circ}\text{C}$. By using the reported method that defining the temperature inducing a half-increase of the total increase in optical absorbance as the LCST of polymer (47), the LCSTs of the copolymers were determined as 28.1, 29.9, 28.3, and 30.2 $^{\circ}\text{C}$ for 1', 2', 3', and 4', respectively. Because of the introduction of hydrophobic cysteamine or HEMA-acrylate units to the polymeric chain of thiol-modified P(NIPAAm-*co*-NAS) or vinyl-modified P(NIPAAm-*co*-HEMA), the copolymers were more hydrophobic, resulting in lower LCSTs in comparison with that of pure PNIPAAm. Moreover, for the same type of copolymer, the LCST got lower as the content of the hydrophobic cysteamine or HEMA-acrylate units increased. For example, because of the higher content of NAS units in 1 than that of 2 (Table 1), the content of hydrophobic cysteamine of 1' was thus higher than that 2', resulting in a lower LCST of 1' in comparison with that of 2'.

In situ Hydrogel Formation via Michael-Type Addition Reaction. When the solutions of thiol-modified P(NIPAAm-*co*-NAS) and vinyl-modified P(NIPAAm-*co*-HEMA) were mixed, vortexed and then placed at 37 $^{\circ}\text{C}$, the expected gelation was observed within one minute (Scheme 2). The detailed gelation process was examined by oscillatory rheology and the corresponding time and temperature sweeps are presented in Figures 3 and 4, respectively. As for the time sweeps, the storage modulus (G') became higher than the loss modulus (G'') within ~ 40 s. It is known that the storage modulus is a property representing the elasticity of a material while loss modulus is property representing the viscosity of a material. The higher storage modulus than loss modulus is an indicator that a real three-dimensional network is formed and a higher storage modulus means a stronger mechanical strength of the network. Therefore, the higher storage modulus than loss modulus revealed in Figure 3 demonstrated the formation of solid like gel materials. Moreover, the gelation process of these hydrogels exhibited a typical biphasic profile. That is, a rapid increase of the storage modulus (within the initial ~ 500 s) followed by a smooth increase. The temperature sweeps in Figure 4 also present the similar gelation behavior as mentioned above. The storage modulus (G') increased rapidly when the external temperature increased from ~ 24 to 32 $^{\circ}\text{C}$ (around the LCSTs of the copolymers). Thereafter, the storage modulus increased smoothly during the following temperature range (away from the LCSTs of the copolymers). However, the

Scheme 2. Illustration of the In situ Formed PNIPAAm-Based Hydrogels



separated aqueous solution of thiol-modified P(NIPAAm-*co*-NAS) (5 wt %) or vinyl-modified P(NIPAAm-*co*-HEMA) (5 wt

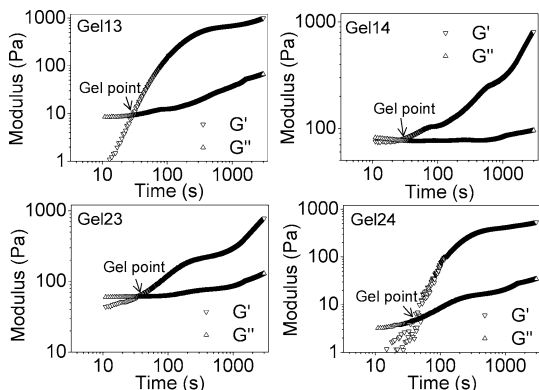


FIGURE 3. Time sweeps of the in situ formed PNIPAAm-based hydrogels (gel point was defined as state that the storage modulus (G') crossed the loss modulus (G'')).

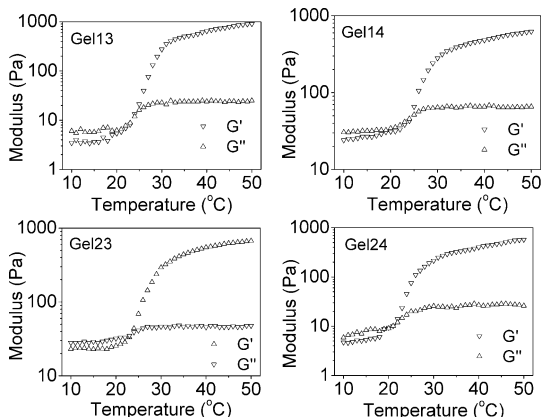


FIGURE 4. Temperature sweeps of the in situ formed PNIPAAm-based hydrogels.

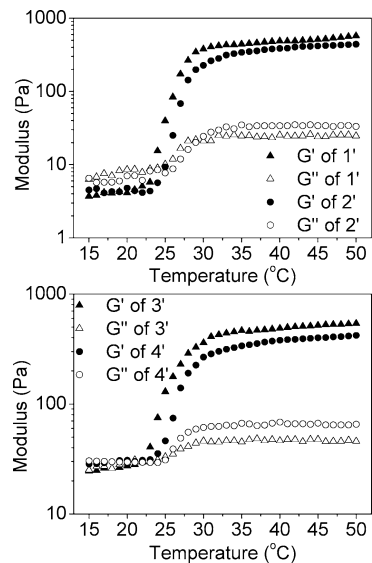


FIGURE 5. Temperature sweeps of thiol-modified P(NIPAAm-*co*-NAS) (1' and 2') and vinyl-modified P(NIPAAm-*co*-HEMA) (3' and 4').

%) did not have such biphasic gelation behavior in their temperature sweeps. As revealed in Figure 5, the storage modulus of the separated copolymer also increased rapidly and became larger than loss modulus when the external temperature ranged from ~ 24 to 32 °C, which can be defined as temperature triggered physical gelation resulting from the rapid aggregation of the copolymer via the hydrophobic interactions of isopropyl groups of NIPAAm units in the polymeric chain (32, 34). However, the storage modulus had no apparent increase and the system reached a stable state when external temperature was higher than ~ 32 °C, indicating that a completely aggregated and collapsed copolymer existed in the formed physical hydrogel.

Combining the information from all the rheology measurements above, the biphasic gelation behavior of these in situ formed hydrogels can be understood. Because the time sweeps of the in situ formed hydrogels were performed at 37 °C, either thiol-modified P(NIPAAm-*co*-NAS) or vinyl-modified P(NIPAAm-*co*-HEMA) can carry out rapid aggregation via the hydrophobic interactions of isopropyl groups of NIPAAm units in the polymeric chains (physical gelation), resulting in a rapid increase of the storage modulus of the hydrogels (32, 34). Even though the presence of the cross-linking reaction between thiol and vinyl functional groups or so-called chemical gelation, the physical gelation of the copolymers was dominate at this stage. As time goes by, especially at the time when the hydrophobic aggregation of PNIPAAm based copolymers accomplished, the cross-linking extent between thiol and vinyl functional groups was enhanced and became dominate, resulting in a continued increase of the storage modulus of the hydrogels. Similarly for the temperature sweeps of these in situ formed hydrogels, the physical gelation of the copolymers at the temperatures around LCSTs induced a rapid increase of the storage modulus. After the complete hydrophobic aggregation of the copolymers, the cross-linking reaction between thiol and vinyl functional groups became dominate, resulting in the increase of the storage modulus.

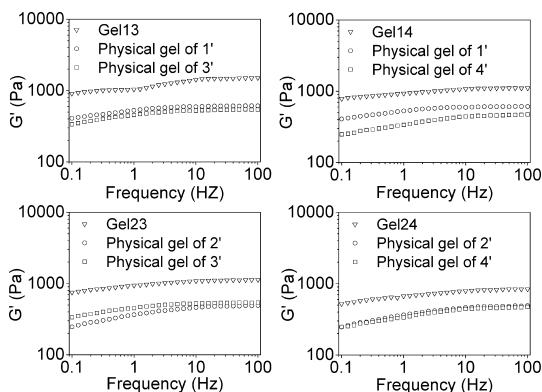


FIGURE 6. Frequency sweeps of the *in situ* formed PNIPAAm based hydrogels and the physical hydrogels of the PNIPAAm based copolymers.

Because physical and chemical gelations occurred during the formation of these *in situ* formed hydrogels, the hydrogels would be physically and chemically cross-linked. Therefore, the mechanical strength of these *in situ* formed hydrogels should be stronger than that of the physical hydrogels of the separated copolymers. The data of the frequency sweeps also demonstrated this point. As exhibited in Figure 6, all the *in situ* formed hydrogels had a higher storage modulus than that of the physical hydrogels of the separated copolymers. In addition, among all these *in situ* formed hydrogels (Table 2), the maximum storage of gel 13 was highest (~ 1506.9 Pa), whereas that of gel 24 was lowest (~ 840.1 Pa), which was attributed to their different cross-linking densities. As shown in Table 1, based on the ^1H NMR spectra, the content of NAS units of P(NIPAAm-*co*-NAS) decreased from **1** to **2**. The corresponding content of thiol functional groups of thiol-modified P(NIPAAm-*co*-NAS) decreased from **1'** to **2'** (Table 2) accordingly. Similarly, the content of vinyl functional groups of vinyl-modified P(NIPAAm-*co*-HEMA) decreased from **3'** to **4'** (Table 2). Therefore, with the equal amounts of thiol-modified P(NIPAAm-*co*-NAS) and vinyl-modified P(NIPAAm-*co*-HEMA), the higher content of thiol and vinyl functional groups for gel 13 can generate a higher cross-linking density, resulting in a higher storage modulus than that of gel 24.

Interior Morphology. Figure 7 displays the interior morphology of the *in situ* formed hydrogels. All the hydrogels had a similar porous network structure. In comparison with the conventional hydrogels with homogeneous network (4, 5), the network structures of these hydrogels were heterogeneous. As described above, the gelation of *in situ* formed hydrogels were performed at $37\text{ }^\circ\text{C}$, which was higher than the LCSTs of thiol-modified P(NIPAAm-*co*-NAS) and vinyl-modified P(NIPAAm-*co*-HEMA). Therefore, during the gelation process, these PNIPAAm-based copolymers can aggregate and precipitate via the hydrophobic interactions of isopropyl groups of NIPAAm units in the polymer chains, resulting in the formation of heterogeneous network structure (6). Actually, preparation of a hydrogel with heterogeneous network structure at a temperature above LCST has been widely used as an efficient strategy to improve the thermal response rates of PNIPAAm based hydrogels (48, 49).

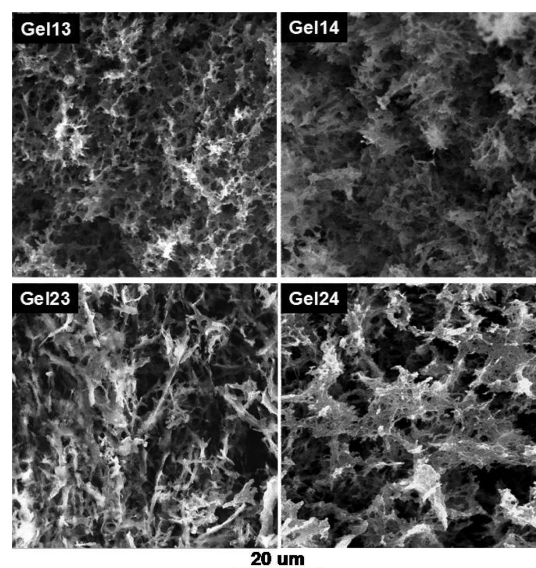


FIGURE 7. SEM images of the *in situ* formed PNIPAAm-based hydrogels.

Moreover, from SEM images in Figure 7, it was found that the average pore sizes of the hydrogels exhibited dependence on their compositions. Because of the higher content of thiol and vinyl functional groups in **1'** and **3'**, the cross-linking density was higher, resulting in lower average pore size of gel 13. In contrary, the lower content of thiol and vinyl functional groups in **2'** and **4'** resulted in larger average pore size of gel 24.

Temperature Dependence of Swelling Ratio.

The temperature dependence of swelling ratio was examined to evaluate the thermal properties of the *in situ* formed hydrogels. The thermosensitivity of the PNIPAAm hydrogel is due to the competition between the intermolecular and intramolecular hydrogen bonding interactions (44–46). At a temperature below LCST, the hydrophilic $\text{C}=\text{O}$ and $\text{N}-\text{H}$ groups in the side chains of the PNIPAAm hydrogel interact easily with water molecules via intermolecular hydrogen bonds. And thus the hydrogel exhibits a hydrophilic and swollen state. When the external temperature is raised, the intermolecular hydrogen bonds are weakened and intramolecular hydrogen bonding interactions between $\text{C}=\text{O}$ and $\text{N}-\text{H}$ groups increase. When the temperature is higher than LCST, the intramolecular hydrogen bonding interactions between $\text{C}=\text{O}$ and $\text{N}-\text{H}$ groups become dominate and result in a compact and collapsed conformation of the PNIPAAm chains. As a result, the hydrogel exhibits a hydrophobic and shrunk state. As exhibited in Figure 8, all the *in situ* formed hydrogels demonstrated the similar thermosensitive profiles described above. Below LCST, all the hydrogels exhibited a swollen state with a higher swelling ratio. For example, swelling ratios of all the samples were above 55 at $5\text{ }^\circ\text{C}$. As the external temperature increased, the swelling ratios decreased and reached the lowest value at $60\text{ }^\circ\text{C}$ (above LCST).

It was found from Figure 8 that the swelling ratios of the hydrogels were different when the external temperature was below LCST. For instance, the swelling ratio of gel 13 was

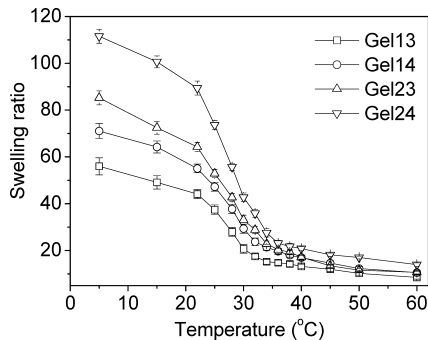


FIGURE 8. Temperature dependence of swelling ratios of the in situ formed PNIPAAm-based hydrogels over the temperature range from 5 to 60 °C.

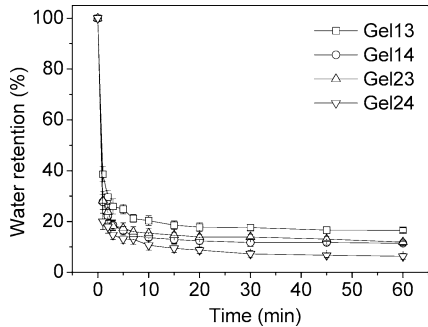


FIGURE 9. Shrinking kinetics of the in situ formed PNIPAAm based hydrogels at 45 °C.

48.9 at 15 °C, whereas those of gel 14, gel 23, and gel 24 was 64.1, 72.1, and 100.8, respectively. This tendency was related to their different cross-linking densities. As shown in Figure 7, the average pore size of gel 13 was lowest while that of gel 24 was largest, resulting in the lowest swelling ratio for gel 13 and the largest swelling ratio for gel 24. It is interesting to note that all the resulted hydrogels present a similar swelling ratio at the temperature above their LCSTs, suggesting that all the hydrogels collapse into a similar network structure.

Shrinking Kinetics at 45 °C. In practical applications, shrinking kinetics at the temperature above LCST is extremely important. Figure 9 presents the shrinking kinetics of the prepared hydrogels after transferring the swollen samples to hot water (above LCST). It was shown that all the hydrogels tended to shrink and lost water once immersed into hot water at 45 °C. All the hydrogels lost at least 75% water within 3 min, which was significantly higher than that of conventional PNIPAAm-based hydrogels (4, 5, 25, 39). The dramatically improved shrinking rates were attributed to the heterogeneous network structures, which accelerated the shrinking rate upon heating. It is accepted that heterogeneous matrix could lead to a fast response rate because of the existence of nonequilibrated shrinking force at different collapsed regions (39, 50). Because of the heterogeneous network structure, numerous shrunk regions appear but with different collapsed phase during the shrinking process. The water-rich regions connect with each other and an interconnected water release channel is generated throughout the hydrogel. As a result, the freed water is evacuated quickly from the collapsing network, inducing a fast response rate

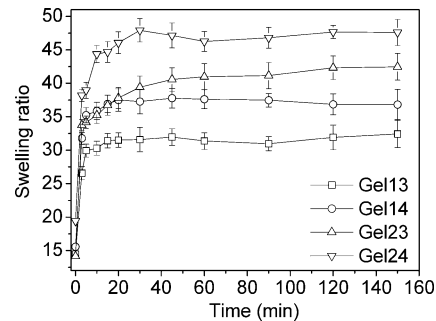


FIGURE 10. Swelling kinetics of the in situ formed PNIPAAm-based hydrogels at 22 °C.

for the hydrogel with heterogeneous network structure. In addition, from the data in Figure 9, all the hydrogels presented different shrinking rates. For example, the water retention of gel 13 decreased from 100% to 17.8% within 20 min, whereas those of gel 14, gel 23, and gel 24 decreased respectively from 100% to 12.4, 13.9, and 8.7% within the same time frame. This tendency is easily understood if their different average pore sizes are taken into account.

Swelling Kinetics at 22 °C. The (re)swelling rate at a decreased temperature (below LCST) is equally critical for its future practical applications, especially used as recyclable intelligent devices. Figure 10 presents the swelling behaviors of the in situ formed hydrogels in distilled water at 22 °C. Because of the different feed compositions resulting in different cross-linking densities of the hydrogels as described above, the corresponding swelling rates of the hydrogels were different with each other. For example, gel 24, which had the largest average pore size, exhibited the fastest swelling rate of all the hydrogels. Its swelling ratio can reach 47.7 within 30 min. On the contrary, because of the lowest average pore size of gel 13, the swelling ratio reached only 31.7 within the same time frame.

In vitro Drug Release. One of the great benefits to use an in situ formed hydrogel for therapeutic delivery is that the therapeutic drugs can be incorporated during the hydrogel formation. This strategy allows precise control over the concentration of the incorporated drug. Gel 13 and gel 24 were selected to assess the influence of thermal stimulus on their drug release profiles. After the gelation in the fish DNA loaded PBS, the encapsulation efficiency was examined as 85.4% for gel 13 and 79.6% for gel 24. From the drug release profiles presented in Figure 11, it was found that either gel 13 or gel 24 exhibited a faster release rate at 37 °C (above the LCSTs of the copolymers) than that at 22 °C (below the LCSTs of copolymers). In detail, at 37 °C, the cumulative release percentages of gel 13 and gel 24 within 40 min were 66.1 and 81.9%, respectively, whereas that at 22 °C was lower and below 55.3% within the same time period. The faster release rate at the temperature above LCST was due to the extra force to expel the loaded drug out during the shrinking process of the hydrogels (4, 39).

In addition, comparing the drug release profile of gel 13 with gel 24, the corresponding release rate was lower at the same temperature. At 22 or 37 °C, around 40.1 or 58.5%

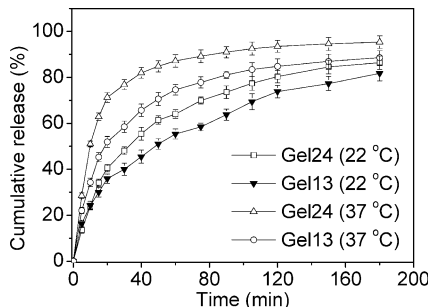


FIGURE 11. Cumulative release of fish DNA from the in situ formed PNIPAAm-based hydrogels at 22 and 37 °C.

loaded fish DNA was released from gel 13 within 30 min, whereas the cumulative release percentage of gel 24 reached 48.2 or 76.9% within the same time interval. It should be noted that the faster release rates of gel 24 than gel 13 at 22 and 37 °C were not attributed to the same reason. At 37 °C, because of the shrinking of the hydrogels, the release rates of the hydrogels were related to the corresponding shrinking rates. As exhibited in Figure 9, the shrinking rate of gel 24 was faster than that of gel 13, resulting in a faster release rate of gel 24 than that of gel 13 at 37 °C. However, at 22 °C, because of gel 13 and gel 24 presenting swollen states, the release rates of the hydrogels were determined by the drug diffusion (39). Therefore, a hydrogel with higher cross-linking density such as gel 13 described above would have a slower drug release rate.

In this study, the data revealed in Figure 11 indicated that at least 80% loaded drug was released from the in situ formed PNIPAAm-based hydrogels within 180 min. From the standpoint of certain applications, these hydrogels might be not suitable for prolonged release systems. However, based on the different drug release profiles upon thermal stimulus, these hydrogels have the potential application in the biomedical fields, especially for some therapeutic drugs such as carbamazepine (51), paracetamol (52), and ibuprofen (53), which need to be released quickly to reach the effective concentration to alleviate the corresponding symptoms.

CONCLUSIONS

A series of in situ formed thermosensitive hydrogels were designed and prepared at physiological temperature (37 °C). Due to the rapid hydrophobic aggregation of the PNIPAAm segments in the polymeric chains (physical gelation) and cross-linking between thiol and vinyl functional groups (chemical gelation), the resulted hydrogels were physically and chemically cross-linked. Simultaneously, because the gelation was carried out at 37 °C, which was higher than the LCSTs of the PNIPAAm-based copolymers, these in situ formed hydrogels had heterogeneous network structures, resulting in an improved thermosensitivity in comparison with the conventional one. The drug release profiles of these hydrogels upon thermal stimulus suggest potential applications in biomedical fields.

Acknowledgment. This work was supported by National Natural Science Foundation of China (20504024, 20774069)

and Ministry of Education of China (Cultivation Fund of Key Scientific and Technical Innovation Project 707043).

REFERENCES AND NOTES

- Bae, Y. H.; Kim, S. W. *Adv. Drug Delivery Rev.* **1993**, *11*, 109–135.
- Okano, T. *Biorelated Polymers and Gels*; Academic Press: San Diago, CA; 1998.
- Gil, E. S.; Hudson, S. M. *Prog. Polym. Sci.* **2004**, *29*, 1173–1222.
- Xu, X. D.; Wei, H.; Zhang, X. Z.; Cheng, S. X.; Zhuo, R. X. *J. Biomed. Mater. Res.* **2007**, *81A*, 418–426.
- Xu, X. D.; Zhang, X. Z.; Yang, J.; Cheng, S. X.; Zhuo, R. X.; Huang, Y. C. *Langmuir* **2007**, *23*, 4231–4236.
- Zhang, X. Z.; Xu, X. D.; Cheng, S. X.; Zhuo, R. X. *Soft Matter* **2008**, *4*, 385–391.
- Zhang, X. Z.; Wu, D. Q.; Chu, C. C. *Biomaterials* **2004**, *25*, 4719–4730.
- Langer, R.; Vacanti, J. P. *Science* **1993**, *260*, 920–926.
- Jeong, B.; Bae, Y. H.; Lee, D. S.; Kim, S. W. *Nature* **1997**, *388*, 860–862.
- Bae, S. J.; Suh, J. M.; Sohn, Y. S.; Bae, Y. H.; Kim, S. W.; Jeong, B. *Macromolecules* **2005**, *38*, 5260–5265.
- Bromberg, L. E.; Ron, E. S. *Adv. Drug Delivery Rev.* **1998**, *31*, 197–221.
- Li, J.; Li, X.; Ni, X. P.; Wang, X.; Li, H. Z.; Leong, K. W. *Biomaterials* **2006**, *27*, 4132–4140.
- Kretschmann, O.; Choi, S. W.; Miyauchi, M.; Tomatsu, I.; Harada, A.; Ritter, H. *Angew. Chem., Int. Ed.* **2006**, *45*, 4361–4165.
- Haines, L. A.; Rajagopal, K.; Ozbas, B.; Salick, D. A.; Pochan, D. J.; Schneider, J. P. *J. Am. Chem. Soc.* **2005**, *127*, 17025–17029.
- Hiemstra, C.; Zhou, W.; Zhong, Z. Y.; Wouters, M.; Feijen, J. *J. Am. Chem. Soc.* **2007**, *129*, 9918–9926.
- Hiemstra, C.; Van Der Aa, L. J.; Zhong, Z. Y.; Dijkstra, P. J.; Feijen, J. *Macromolecules* **2007**, *40*, 1165–1173.
- Halstenberg, S.; Panitch, A.; Rizzi, S.; Hall, H.; Hubbell, J. A. *Biomacromolecules* **2002**, *3*, 710–723.
- Nguyen, K. T.; West, J. L. *Biomaterials* **2002**, *23*, 4307–4314.
- Zhu, J. M.; Beamish, J. A.; Tang, C.; Kottke-Marchant, K.; Marcant, R. E. *Macromolecules* **2006**, *39*, 1305–1307.
- Luo, Y.; Kirker, K. R.; Prestwich, G. D. *J. Controlled Release* **2000**, *69*, 169–184.
- Jia, X.; Colombo, G.; Padera, R.; Langer, R.; Kohane, D. S. *Biomaterials* **2004**, *25*, 4797–4804.
- Tam, J. P.; Xu, J.; Eom, K. D. *Biopolymers* **2001**, *60*, 194–205.
- Wang, Z. C.; Xu, X. D.; Chen, C. S.; Wang, G. R.; Cheng, S. X.; Zhang, X. Z.; Zhuo, R. X. *React. Funct. Polym.* **2009**, *69*, 14–19.
- Ossipov, D. A.; Hilborn, J. *Macromolecules* **2006**, *39*, 1709–1718.
- Xu, X. D.; Chen, C. S.; Wang, Z. C.; Wang, G. R.; Cheng, S. X.; Zhang, X. Z.; Zhuo, R. X. *J. Polym. Sci., Part A: Polym. Chem.* **2008**, *46*, 5263–5277.
- Xu, X. D.; Chen, C. S.; Lu, B.; Wang, Z. C.; Cheng, S. X.; Zhang, X. Z.; Zhuo, R. X. *Macromol. Rapid Commun.* **2009**, *30*, 157–164.
- Elbert, D. L.; Pratt, A. B.; Lutolf, M. P.; Halstenberg, S.; Hubbell, J. A. *J. A. J. Controlled Release* **2001**, *76*, 11–25.
- Lutolf, M. P.; Hubbel, J. A. *Biomacromolecules* **2003**, *4*, 713–722.
- Lutolf, M. P.; Raeber, G. P.; Zisch, A. H.; Tirelli, N.; Hubbell, J. A. *Adv. Mater.* **2003**, *15*, 888–892.
- Hiemstra, C.; van der Aa, L. J.; Zhong, Z. Y.; Dijkstra, P. J.; Feijen, J. *Biomacromolecules* **2007**, *8*, 1548–1556.
- Qiu, B.; Stefanos, S.; Ma, J.; Lalloo, A.; Perry, B. A.; Leibowitz, M. J.; Sisko, P. J.; Stein, S. *Biomaterials* **2003**, *24*, 11–18.
- Lee, B. H.; West, B.; McLemore, R.; Pauken, C.; Vernon, B. L. *Biomacromolecules* **2006**, *7*, 2059–2064.
- Hahn, S. K.; Oh, E. J.; Miyamoto, H.; Shimobouji, T. *Int. J. Pharm.* **2006**, *322*, 44–51.
- Robb, S. A.; Lee, B. H.; McLemore, R.; Vernon, B. L. *Biomacromolecules* **2007**, *8*, 2294–2300.
- Torres-Lugo, M.; Peppas, N. A. *Macromolecules* **1999**, *32*, 6646–6651.
- Hoffman, A. S. *J. Controlled Release* **1987**, *6*, 297–305.
- Suzuki, A.; Tanaka, T. *Nature* **1990**, *346*, 345–347.
- Stayton, P. S.; Shimobouji, T.; Long, C.; Chilkoti, A.; Chen, G. H.; Harris, J. M.; Hoffman, A. S. *Nature* **1995**, *378*, 472–474.
- Xu, X. D.; Wang, B.; Wang, Z. C.; Cheng, S. X.; Zhang, X. Z.; Zhuo, R. X. *J. Biomed. Mater. Res.* **2008**, *86 A*, 1023–1032.
- Liu, F.; Tao, G. L.; Zhuo, R. X. *Polym. J.* **1993**, *25*, 561–567.

(41) Dong, L. C.; Hoffman, A. S. *J. Controlled Release* **1990**, *13*, 21–31.

(42) Bae, Y. H.; Okano, T.; Kim, S. W. *Pharm. Res.* **1991**, *8*, 531–537.

(43) Qiu, Y.; Park, K. *Adv. Drug Delivery Rev.* **2001**, *53*, 321–339.

(44) Zhang, X. Z.; Wu, D. Q.; Chu, C. C. *Biomaterials* **2004**, *25*, 3793–3805.

(45) Xu, X. D.; Zhang, X. Z.; Cheng, S. X.; Zhuo, R. X. *Colloid Polym. Sci.* **2006**, *285*, 75–82.

(46) Xu, X. D.; Zhang, X. Z.; Wang, B.; Cheng, S. X.; Zhuo, R. X.; Wang, Z. C. *Colloid. Surf., B* **2007**, *59*, 158–163.

(47) Chang, C.; Wei, H.; Quan, C. Y.; Li, Y. Y.; Liu, J.; Wang, Z. C.; Cheng, S. X.; Zhang, X. Z.; Zhuo, R. X. *J. Polym. Sci., Part A: Polym. Chem.* **2008**, *46*, 3048–3057.

(48) Zhang, X. Z.; Zhuo, R. X. *J. Colloid Interface Sci.* **2000**, *223*, 311–313.

(49) Takata, S.; Suzuki, K.; Norisuye, T.; Shibayama, M. *Polymer* **2002**, *43*, 3101–3107.

(50) Okajima, T.; Harada, I.; Nishio, K.; Hirotsu, S. *J. Chem. Phys.* **2002**, *116*, 9068–9077.

(51) Perissutti, B.; Rubessa, F.; Moneghini, M.; Voinovich, D. *Int. J. Pharm.* **2003**, *256*, 53–63.

(52) Abdelbary, G.; Prinderre, P.; Eouani, C.; Joachim, J.; Reynier, J. P.; Piccerelle, P. *Int. J. Pharm.* **2004**, *278*, 423–433.

(53) Passerini, N.; Albertini, B.; Gonzalez-Rodriguez, M. L.; Cavallari, C.; Rodriguez, L. *Eur. J. Pharmacol.* **2002**, *15*, 71–78.

AM900712E